



SEE WHAT  
YOU'VE BEEN MISSING

ADVANCED FLOW CYTOMETRY  
THAT REVEALS UP TO 40 COLORS

LEARN MORE



## The Human IL-2 Gene Promoter Can Assemble a Positioned Nucleosome That Becomes Remodeled Upon T Cell Activation

This information is current as of October 22, 2019.

Joanne L. Attema, Raymond Reeves, Vincent Murray, Ilya Levichkin, Mark D. Temple, David J. Tremethick and M. Frances Shannon

*J Immunol* 2002; 169:2466-2476; ;  
doi: 10.4049/jimmunol.169.5.2466  
<http://www.jimmunol.org/content/169/5/2466>

**References** This article **cites 63 articles**, 31 of which you can access for free at:  
<http://www.jimmunol.org/content/169/5/2466.full#ref-list-1>

Why *The JI*? [Submit online.](#)

- **Rapid Reviews! 30 days\*** from submission to initial decision
- **No Triage!** Every submission reviewed by practicing scientists
- **Fast Publication!** 4 weeks from acceptance to publication

*\*average*

**Subscription** Information about subscribing to *The Journal of Immunology* is online at:  
<http://jimmunol.org/subscription>

**Permissions** Submit copyright permission requests at:  
<http://www.aai.org/About/Publications/JI/copyright.html>

**Email Alerts** Receive free email-alerts when new articles cite this article. Sign up at:  
<http://jimmunol.org/alerts>

*The Journal of Immunology* is published twice each month by  
The American Association of Immunologists, Inc.,  
1451 Rockville Pike, Suite 650, Rockville, MD 20852  
Copyright © 2002 by The American Association of  
Immunologists All rights reserved.  
Print ISSN: 0022-1767 Online ISSN: 1550-6606.



# The Human IL-2 Gene Promoter Can Assemble a Positioned Nucleosome That Becomes Remodeled Upon T Cell Activation<sup>1</sup>

Joanne L. Attema,\* Raymond Reeves,<sup>†</sup> Vincent Murray,<sup>‡</sup> Ilya Levichkin,<sup>2\*</sup> Mark D. Temple,<sup>‡</sup> David J. Tremethick,\* and M. Frances Shannon<sup>3\*</sup>

Controlled production of the cytokine IL-2 plays a key role in the mammalian immune system. Expression from the gene is tightly regulated with no detectable expression in resting T cells and a strong induction following T cell activation. The IL-2 proximal promoter (+1 to -300) contains many well-defined transcriptional activation elements that respond to T cell stimulation. To determine the role of chromatin structure in the regulation of interleukin-2 gene transcription, nucleosome assembly across the IL-2 promoter region was examined using in vitro chromatin reconstitution assays. The IL-2 promoter assembles a nucleosome that is both translationally and rotationally positioned, spanning some of the major functional control elements. The binding of transcription factors to these elements, with the exception of the architectural protein HMGA1, was occluded by the presence of the nucleosome. Analysis of the chromatin architecture of the IL-2 gene in Jurkat T cells provided evidence for the presence of a similarly positioned nucleosome in vivo. The region encompassed by this nucleosome becomes remodeled following activation of Jurkat T cells. These observations suggest that the presence of a positioned nucleosome across the IL-2 proximal promoter may play an important role in maintaining an inactive gene in resting T cells and that remodeling of this nucleosome is important for gene activation. *The Journal of Immunology*, 2002, 169: 2466–2476.

The generation of T cell-mediated immune responses is critically regulated by the coordinate expression of cytokine genes. A key event in the initial activation of T cells upon Ag exposure is the production of the cytokine IL-2 and its high affinity receptor (IL-2R) comprising  $\alpha$ ,  $\beta$ , and  $\gamma$  subunits (reviewed in Ref. 1). Together they form a strong autocrine loop for promoting T cell growth and clonal expansion, and possibly contributing to B cell differentiation, macrophage, and NK cell activation (2). High levels of IL-2 are produced when T cells are activated through both the Ag-specific TCR interacting with peptide:MHC complexes on APCs and costimulatory interactions such as B7 on APCs with CD28 receptors on T cells (3). IL-2 is necessary for the generation of correct immune responses, as indicated by the fact that IL-2-deficient mice develop a thymic disorder that disrupts thymocyte development (4). Other conditions such as hemolytic anemia, chronic inflammatory bowel disease, and severe autoimmunity are also prevalent in IL-2-deficient mice leading to the conclusion that IL-2 plays a critical role in T cell homeostasis (5).

Transcription from the IL-2 gene is highly inducible following Ag stimulation of T cells and is further enhanced by cross-linking

costimulatory CD28 receptors with an anti-CD28 Ab (6–8). The regulatory regions of the human IL-2 promoter have been studied in detail and it was initially established that ~300 nt upstream from the start of transcription was sufficient for maximal activity in transient transfection assays in Jurkat T cells (9, 10). Within this minimal promoter region, two major TCR responsive regions were identified in the human gene and termed Ag-responsive elements (ARRE),<sup>4</sup> ARRE-1 and ARRE-2 (Ref. 11; see Fig. 1). The binding of AP-1 and NF-AT as well as Oct transcription factors controls both ARRE-1 and ARRE-2 (12–17). Another important site within the IL-2 minimal promoter is a region that responds to CD28 costimulation, known as the CD28 response region (RR) (8, 18, 19) (see Fig. 1). This region contains a CD28 response element (RE) that is a variant NF- $\kappa$ B site and binds RelA homodimers and c-Rel-containing complexes as well as NFAT proteins (8, 18–23). The CD28RR also contains an AP-1 transcription factor-binding site that functions cooperatively with the CD28RE (24). Although controversy exists concerning the AP-1 proteins that operate on this site, ATF-2/CREB bZIP proteins and *c-fos* and *c-jun* AP-1 family members have been shown to bind (24–26).

The architectural protein, HMG-I(Y) (recently renamed HMGA1; Ref. 27) also binds to the CD28RE and its functional importance at the IL-2 promoter has been determined by antisense reporter assays (20). Furthermore, the binding of HMGA1 to the CD28RR has differential effects on NF- $\kappa$ B, NF-AT, and AP-1 interactions at this region (20, 28). For example, HMGA1 selectively promotes binding of both c-Rel and AP-1-containing complexes to the CD28RE whereas the binding of NF-AT is inhibited by HMGA1 (23). These findings have led to the suggestion that HMGA1 plays an important regulatory role in the formation of transcription factor complexes on the CD28RR (28).

\*Division of Molecular Bioscience, John Curtin School of Medical Research, Australian National University, Canberra, Australian Capital Territory, Australia; <sup>†</sup>School of Molecular Bioscience, Washington State University, Pullman, WA 99164; and <sup>‡</sup>School of Biochemistry and Molecular Genetics, University of New South Wales, Sydney, New South Wales, Australia

Received for publication April 25, 2002. Accepted for publication June 20, 2002.

The costs of publication of this article were defrayed in part by the payment of page charges. This article must therefore be hereby marked *advertisement* in accordance with 18 U.S.C. Section 1734 solely to indicate this fact.

<sup>1</sup> Portions of this work were supported by National Institutes of Health Grant No. R01 GM 46352 (to R.R.). Funding from National Health and Medical Research Council (Australia) and Boehringer Ingelheim (to M.F.S.) also supported this work. J.L.A. was supported by an Australian National University postgraduate scholarship.

<sup>2</sup> Current address: School of Biochemistry, LaTrobe University, Melbourne, Victoria, Australia.

<sup>3</sup> Address correspondence and reprint requests to Dr. M. Frances Shannon, Division of Molecular Bioscience, John Curtin School of Medical Research, Australian National University, Canberra, Australian Capital Territory, 2601, Australia. E-mail address: frances.shannon@anu.edu.au

<sup>4</sup> Abbreviations used in this paper: ARRE, Ag-responsive element; RR, response region; RE, response element; MNase, micrococcal nuclease; RT, room temperature; LM, ligation-mediated; BLM, bleomycin sulfate; CHART-PCR, chromatin accessibility using real-time PCR; NF-ATp, preexisting NF-AT.

The association of these transcription factors with the IL-2 promoter occurs in the context of chromatin within the nucleus. Alterations in the chromatin structure of the promoter/enhancer regions of inducible genes are thought to play an important role in regulating their transcription (29–31). A number of mechanisms govern chromatin remodeling events including transient modification and subsequent destabilization of the nucleosomal structure by histone acetylases, nucleosome sliding, dissociation of some core histones, or stable disruption leading to nucleosome-free regions (32–36). DNase I digestion, restriction enzyme accessibility assays, and *in vivo* genomic footprinting analyses have been used to probe the chromatin structure of the promoter region of the IL-2 gene before and after its transcriptional activation in human and mouse T lymphocytes. These experiments revealed that in resting mouse and human T cells, when the IL-2 gene is silent, the proximal promoter region is inaccessible to DNase I and restriction enzyme digestion. Following stimulation, new DNase I hypersensitive sites appear suggesting changes in chromatin structure (37–41).

In this study, we report that the IL-2 proximal promoter has the intrinsic capacity to assemble a precisely positioned nucleosome *in vitro* and present evidence that a similarly positioned nucleosome exists *in vivo*. This nucleosome prevents transcription factor binding *in vitro* and appears to be transiently remodeled following T cell activation.

## Materials and Methods

### *Production and purification of recombinant proteins*

Recombinant hexahistidine-tagged full-length Fos and Jun proteins, as well as truncated Fos 116–211 and Jun 224–334 proteins, were prepared and purified by affinity chromatography using a Ni-NTA-agarose column (Qiagen, Valencia, CA) as previously described (42). Fos and Jun proteins were co-renewed *in vitro* into the heterodimer transcription factor AP-1 by step-wise dialysis from 6 M urea with the final buffer containing 25 mM sodium phosphate, pH 7.6, 5% glycerol, and 5 mM DTT (34). Full-length recombinant wild-type human HMG1 proteins (i.e., HMG1a and HMG1b, formerly called HMG-I and HMG-Y, respectively; Ref. 27), and the HMG1-MII, MIII mutant protein, were produced as described elsewhere (43, 44). NF-ATp and c-Rel were prepared as previously described (20, 23). The purity of each recombinant preparation was assessed by SDS-PAGE (44).

### *Cell culture and stimulation*

Human Jurkat T leukemia cells were maintained in RPMI 1640 medium supplemented with 10% FCS and the antibiotics, gentamicin and penicillin. Approximately  $2.5 \times 10^7$  Jurkat T cells were stimulated using 20 ng/ml of PMA and 1  $\mu$ M calcium ionophore. Bristol-Myers Squibb (Seattle, WA) supplied the activating CD28 mAb (WA93165) used at a 1/10,000-fold dilution.

### *Chromatin reconstitution and characterization of nucleosome rotational settings*

Histones were reconstituted onto radiolabeled IL-2 promoter fragments by high-salt to low-salt step-wise exchange with 30- to 60-fold excess of either isolated chicken erythrocyte nucleosome core particles or H1-depleted oligonucleosomes as previously described (41, 45). The *in vitro*-reconstituted nucleosomes were routinely purified from both contaminating free DNA and unbound proteins by loading onto a pre-equilibrated 5–20% 10 ml sucrose gradient in buffer containing 1 M Tris, pH 7.5, 500 mM EDTA, and 100 mM PMSF and centrifuged at 4°C for 16 h at 35,000 rpm. Nucleosome-containing fractions were determined by PAGE, pooled, and then dialysed in a buffer of 10 mM Tris pH 7.5, 1 mM EDTA, and 1 mM 2-ME for 16 h. Following dialysis, the nucleosome preparation was concentrated to a volume of 400  $\mu$ l using Amicon-30 MW columns (Beverly, MA).

### *Determination of the boundaries of translationally positioned nucleosomes*

The approximate 5' and 3' boundaries of nucleosomes that are translationally positioned on a PCR-generated 220-bp fragment of IL-2 promoter DNA reconstituted into chromatin *in vitro* (see Fig. 2F) were determined by previously described methods (46). Briefly, the reconstituted chromatin

was digested with micrococcal nuclease (MNase; Boehringer Mannheim, Indianapolis, IN) to release monomer nucleosome core particles (containing ~146–150 bp of DNA). The quality of the released core particles was routinely monitored by analyzing their electrophoretic mobility on native nucleoprotein gels, by SDS-PAGE analysis of their histone protein content and by analysis of the sizes of the DNA fragments by electrophoretic separations on 6% denaturing polyacrylamide sequencing gels. Monomer nucleosome-length DNA was purified from the core histone proteins and enzymatically  $^{32}$ P-labeled on both its 5' ends using T4 polynucleotide kinase (New England Biolabs, Beverly, MA) and the resulting fragment digested with restriction endonucleases (e.g., *MseI*, *HinfI*, *SspI*; see Fig. 2F) to determine whether their recognition sites were present within the fragments. The sizes of the released radiolabeled DNA subfragments indicate the distance from cut site to the 5' and 3' borders of the core particle (see Fig. 2F).

### *EMSA*

Purified recombinant AP-1, c-Rel, preexisting NF-AT (NF-ATp), and HMG1 were incubated for 5 min at room temperature (RT) in a buffer with final concentrations of 10 mM Tris, pH 7.5, 10 mM MgCl<sub>2</sub>, 5 mM EDTA, 10 mM DTT, 0.2% Nonidet P-40, 1% glycerol, 0.4% sucrose, 0.5 mg/ml BSA, and 100 ng of poly(dG:dC) in 20  $\mu$ l. Either radiolabeled nucleosome-assembled IL-2 (0.1 ng) or free DNA (0.1 ng) was used with indicated amounts of proteins for each experiment and incubated at RT for 20 min, before the reactions were separated on 5% 1 $\times$  Tris-borate EDTA polyacrylamide gels. Gels were dried and exposed to x-ray film or phosphorimager intensifying screens. Digital images were produced on a Fuji LAS 3000 phosphorimager and analyzed with ImageGauge software (Fuji, Tokyo, Japan).

### *DNase I and hydroxyl radical footprinting*

Promoter fragments were 5'-end radiolabeled by T4 polynucleotide kinase and [ $\gamma$ - $^{32}$ P]ATP. Footprinting of HMG1 recombinant proteins on promoter DNA fragments radiolabeled on only one 5' end using the nuclease DNase I followed detailed published protocols (43, 47). For each protein and DNA substrate, optimal conditions for footprinting were empirically determined. ssDNA cleavage products were then separated by electrophoresis on 6% sequencing gels with Maxam-Gilbert "G+A" chemical cleavage products of control DNA fragments serving as a reference standard. Band intensities were quantified using a Fuji phosphorimager and ImageGauge software (Fuji). Hydroxyl radical cleavage of both free IL-2 promoter DNA and *in vitro* reconstituted chromatin substrates followed published procedures (46, 48).

### *Analysis of chromatin by ligation-mediated (LM)-PCR*

Cells ( $2.5 \times 10^7$ ) were washed in PBS and resuspended at a final concentration of  $5 \times 10^6$  cells/ml containing 0.5 to 2 mM bleomycin sulfate (BLM) (Blenoxane; Bristol-Myers Squibb). After a 30-min incubation at 37°C, the suspension was centrifuged to pellet the cells, the supernatant was removed, and the cell pellet was resuspended in 200  $\mu$ l of PBS. Genomic DNA was prepared using the Qiagen Genomic DNA purification columns. LM-PCR was performed as previously described (49, 50) using IL-2-specific oligonucleotides (Table I). Following LM-PCR, 4  $\mu$ l of each sample was combined with 4  $\mu$ l of sequencing loading dye and electrophoresed on 6% (w/v) polyacrylamide sequencing gels. Gels were vacuum-dried on DEAE-3 chromatography paper, exposed to phosphorimager screens (Fuji), and scanned using a Fuji phosphorimager. Image analysis was performed using ImageGauge software.

### *Chromatin accessibility using real-time PCR (CHART-PCR)*

MNase and restriction enzyme accessibility assays were performed as recently described (51). Briefly, Jurkat T cell nuclei were resuspended in either MNase digestion buffer (10 mM Tris, pH 7.5, 15 mM NaCl, 60 mM KCl, 1 mM CaCl<sub>2</sub>) or restriction enzyme buffer (1 $\times$  buffer supplied by New England Biolabs (1  $\mu$ l of 2 mg/ml leupeptin, 1  $\mu$ l of 1.8 mg/ml aprotinin, and 1  $\mu$ l of 100 mM PMSF)) and incubated with the appropriate endonuclease. Reactions were stopped with the addition of EDTA to 20 mM final concentration. A control without the accessibility agent was included from both the stimulated and unstimulated cells to monitor for endonuclease activity. Isolated genomic DNA (50 ng) was used to perform SYBR green real-time PCR as recently described (51). The amplicon length was kept between 100 and 200 bp. Identical thermocycler conditions were used for all primer sets: stage 1, 50°C/2 min for 1 cycle; stage 2, 95°C/10 min for 1 cycle; stage 3, 95°C/15 s, 60°C/1 min

Table I. Oligonucleotide sequences of the primers used in LM-PCR and CHART-PCR assays

Primer Set	Oligonucleotide Sequence	Melting Temperature (°C)
LM-PCR oligonucleotides		
A		
11	5'-TGTTTACTCTTGCTCTGTCCACCAC-3'	60
12	5'-TTGTCCACCACAATATGCTATTTCAC-3'	60.5
13	5'-CACATGTTTCAGTGTAGTTTTATGAC-3'	61
B		
56	5'-CACCTAAGTGTGGGCTAATGTAAC-3'	60
57	5'-AACAAAAGAGGGATTTCACCTACATCC-3'	61
58	5'-TTCACCTACATCCATTTCAGTCAGTC-3'	62
Linker Bottom	5'-GAAGAGAAGGT-3'	
Linker Top	5'-CCAAACGCCATTTCCACCTTCTCTTC-3'	
CHART-PCR oligonucleotides		
A		
Coding	5'-CGTTAAACAGTACCTCAAGCTCAA-3'	
Noncoding	5'-CCTTTTATCCACACAAAAGAGCTA-3'	
B		
Coding	5'-GGGCTAATGTAACAAAGAGGGATT-3'	
Noncoding	5'-AACCCATTTTCTCTTCTGATGA-3'	
C		
Coding	5'-CTACTCACAGTAACCTCAACTCCT-3'	
Noncoding	5'-TGTAGAACTTGAAGTAGGTGCACT-3'	

for 40 cycles. To correlate the Ct values (threshold values) from the IL-2 CHART-PCR amplification plots to percent accessibility, a standard curve was generated using serial dilutions of genomic DNA and the appropriate primer sets.

## Results

### The IL-2 proximal promoter reconstitutes rotationally and translationally positioned nucleosomes *in vitro*

To determine whether the establishment of a precise chromatin architecture, consisting of positioned nucleosomes, plays a role in the inducible expression of the human IL-2 gene, 5' end-labeled, IL-2 promoter DNA fragments (Fig. 1) were reconstituted into nucleosomes *in vitro* (52). A 180-bp fragment corresponding to the region of the IL-2 promoter from nt -55 to -235 (see Fig. 1) formed a distinct shifted complex upon addition of increasing amounts of chicken donor chromatin (Fig. 2A, lanes 2-4) suggesting that this portion of the IL-2 promoter can assemble into a discrete mononucleosome. A longer IL-2 promoter fragment from

nt -320 to +40 (360 bp; Fig. 1) also assembled into one major band (Fig. 2A) suggesting discrete nucleosome positions. In contrast to the IL-2 promoter, a 240-bp fragment (-200 to +40) from the GM-CSF promoter gave rise to several shifted complexes following nucleosome assembly (Fig. 2B, lanes 2-4). The fine structure of the *in vitro* nucleosome reconstitutes was analyzed by a variety of high-resolution mapping techniques to determine whether the *in vitro* assembled core particles had assumed distinct translational and/or rotational positions with respect to the underlying DNA sequences. DNase I cleavage of the 180-bp (nt -55 to -235) IL-2 mononucleosome complex revealed a pronounced periodic pattern of hypersensitive bands distinct from that of naked DNA (Fig. 2C, compare lanes 2-5 with 6-9) suggesting that a rotationally positioned nucleosome is assembled on IL-2 promoter DNA. In contrast, digestion of the nucleosome-assembled GM-CSF gene promoter did not yield a periodic DNase I digestion pattern (Fig. 2D, compare lanes 8-15 with 1-6) suggesting that

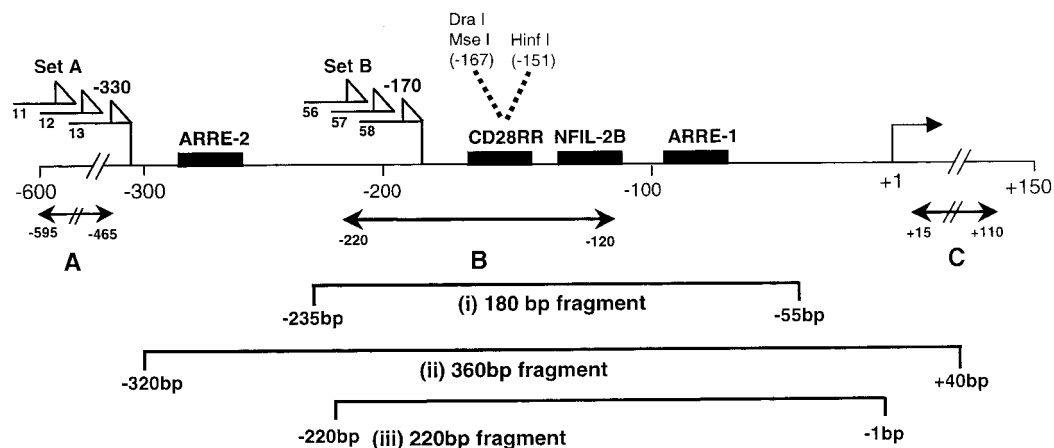


**FIGURE 1.** Schematic of the IL-2 promoter. The IL-2 gene from the coding region (+150) to the distal promoter (-600) is shown. Black bars represent functional transcription factor binding sites and the designated names of the elements are shown. LM-PCR primer set locations are indicated by flagged lines (set A and set B) and restriction enzyme sites used in this study are indicated. Real-time PCR products (arrowed lines) are shown as A, B, and C and the 5' and 3' sequences of each primer set are given in Table I. Below the promoter region schematic, the IL-2 promoter fragments used for *in vitro* reconstitution of nucleosomes are shown.

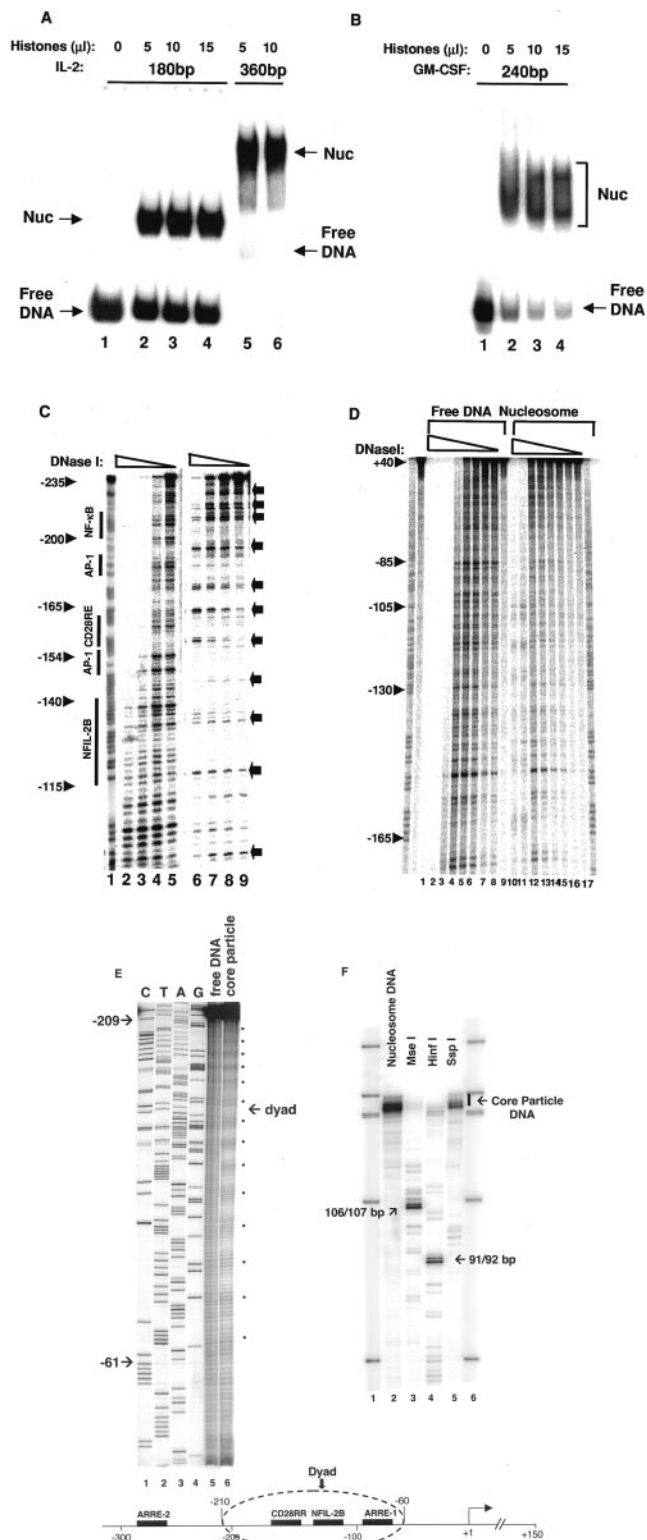


**FIGURE 2.** Reconstitution of IL-2 and GM-CSF promoter fragments into nucleosomes in vitro. *A*, The IL-2 promoter assembles nucleosomes in vitro. Assembly reactions contained the H1-depleted chicken chromatin extracts and 1 ng of radiolabeled 180-bp IL-2 promoter DNA. One-twentieth of the assembly reactions were resolved on nondenaturing 5% polyacrylamide gels. Lanes 1–4 contained 0, 5, 10, and 15  $\mu$ l of the chromatin extract, respectively. Lanes 5 and 6 contain 5 and 10  $\mu$ l chromatin extract with a 360-bp IL-2 fragment. The positions of the nucleosome complexes (Nuc) and free DNA are indicated. *B*, Assembly of nucleosome complexes on the GM-CSF promoter in vitro. A GM-CSF promoter DNA fragment (nt –200 to +40) was assembled into nucleosomes as described in *A*.

this rotational positioning seen for IL-2 was not a general property of all DNA fragments.

To further define the rotational position of the nucleosome(s) on the IL-2 promoter, hydroxyl radical cleavage was performed. Fig. 2*E* shows the results of hydroxyl radical cleavage analysis of a 220-bp fragment of the IL-2 promoter between nt –1 to –220 (Fig. 1) reconstituted into a mononucleosomal particle. Whereas a nearly uniform pattern of cleavages is observed for the naked DNA fragment (Fig. 2*E*, lane 5), the DNA in the reconstituted nucleosome exhibits a pronounced pattern of bands spaced at ~10-bp intervals (indicated by dots adjacent to lane 6 in Fig. 2*E*). This pattern of bands ends at approximately nt 61 where it reverts to the pattern for naked DNA (Fig. 2*E*, lane 6). Consistent with the DNase I cleavage analysis, this periodic pattern of hydroxyl radical cleavage indicates that a rotationally positioned nucleosome is present on IL-2 promoter DNA and that one end of the core particle may be located at approximately nt 61. Interestingly, this nucleosome may function as a boundary nucleosome because using the longer 360-bp fragment of the IL-2 promoter we have found that additional closely packed nucleosomes are positioned upstream of the one located at –61 (data not shown).

To further investigate the stability of the rotationally positioned nucleosome ending at approximately nt 60, restriction enzyme mapping experiments were performed to determine whether it also exhibited a strong translational setting on the promoter DNA. Digestion of MNase-released nucleosomal DNA with *Mse*I releases a distinct 106/107-bp doublet of labeled fragments (Fig. 2*F*, lane

Lanes 1–4 contain 0, 5, 10, and 15  $\mu$ l of chromatin extract, respectively. *C*, DNase I cleavage of the IL-2 promoter assembled into nucleosome. The 180-bp radiolabeled fragment as either free DNA or assembled into a nucleosome was subjected to DNase I cleavage and the resultant DNA fragments were separated using 6% sequencing gels. Increasing concentrations of DNase I were added to free IL-2 promoter DNA (lanes 2–5) and DNA reconstituted into chromatin in vitro (lanes 6–9). Lane 1 shows the G + A sequencing of the 180-bp fragment. The functional transcription factor binding sites are indicated as vertical lines to the left of the G + A marker and the sequence positions relative to the transcription start site at +1 are also shown. The solid arrows indicate the positions of DNase I cleavage sites spaced with an ~10-bp periodicity indicative of a rotationally positioned nucleosome. *D*, DNase I cleavage of the GM-CSF promoter assembled into nucleosome. A 240-bp GM-CSF promoter DNA fragment present as either nucleosomal or free DNA was analyzed as described above (Fig. 2*C*) using DNase I footprinting. Lanes 1–9 contain free DNA and nucleosomal DNA is in lanes 10–17. G + A sequencing lanes are shown at each end of the gel. *E*, Nucleosomes reconstituted onto the IL-2 promoter are rotationally positioned. Hydroxyl radical cleavage mapping of the fine structure of a monomer nucleosome reconstituted onto a 3'-end labeled 221-bp promoter fragment. Lanes 1–4, Sanger sequencing lanes (C, T, A, G) of the IL-2 promoter DNA; lane 3, hydroxyl radical cleavage of free promoter DNA; lane 4, hydroxyl radical cleavage of DNA reconstituted into a nucleosome core particle. The solid dots indicate the position of hydroxyl radical cleavages spaced with an ~10-bp periodicity indicative of a rotationally positioned nucleosome. Nucleotide numbering of the IL-2 promoter sequence is shown on the left. *F*, Defining the borders of the translationally positioned nucleosome reconstituted onto IL-2 promoter DNA. Restriction enzyme cleavage analysis of a monomer nucleosome reconstituted onto a 221-bp fragment of the IL-2 promoter. The lanes correspond to mononucleosome DNA that has not been digested with restriction enzymes (lane 2), or has been digested with *Mse*I (lane 3), *Hinf*I (lane 4), or *Ssp*I (lane 5). Molecular weight markers (in base pair) are shown in lanes 1 and 6. The major digestion products from the restriction enzyme digestions and the core particle DNA are indicated. The diagram at the bottom shows the location of the strongly positioned nucleosome (dashed ellipse) between approximately nt –60 and –210 that can be reconstituted onto the IL-2 promoter in vitro. The dyad axis of the positioned nucleosome is indicated by the arrow.

3) whereas digestion with *HinfI* releases a 91/92-bp doublet (Fig. 2F, lane 3). In the lower part of this gel are additional distinct doublet cleavage bands of 42/43 bp for the *MseI* digest and 57/58 bp for the *HinfI* digest (data not shown). The sizes of the restriction fragments released by these two enzymes indicate that the positioned nucleosome adopts a single highly preferred translational setting on the proximal IL-2 promoter between nt -60/-61 and -208/-209 (Fig. 2F). In contrast, the *SspI* enzyme does not cleave the MNase-released nucleosomal DNA (Fig. 2F, lane 5) because its cut site at nt -52 lies outside of the positioned core particle, thus confirming the results of hydroxyl radical cleavage. Because the prominent DNA fragments released by both restriction enzymes are doublet bands that differ by only a single base pair in size, we attribute these size differences to variations in the extent of MNase trimming of the original chromatin reconstitute.

These data clearly indicate that the IL-2 promoter DNA has the intrinsic ability to assemble a very stable nucleosome core particle that is both rotationally and translationally positioned between nt -60 and -210 encompassing promoter regions that are critical for inducible expression of the IL-2 gene (Fig. 2F).

*The positioned IL-2 nucleosome blocks transcription factor, but not HMGA1, binding to the CD28RR in vitro*

The CD28RR of the IL-2 promoter lies close to the dyad of the positioned nucleosome and has been shown to bind the transcription factors, c-Rel, RelA, AP-1 (*c-fos/c-jun*), and NF-ATp, as well as the architectural protein HMGA1 (20, 21, 23, 25, 28). To determine whether the presence of the nucleosome affected the ability of these transcription factors to gain access to their binding sites, increasing amounts of recombinant transcription factors were added alone or in combination to IL-2 nucleosomes or naked DNA and the resultant complexes were analyzed by EMSA. The addition of increasing amounts of recombinant full-length *c-fos/c-jun* heterodimers (AP-1) (Fig. 3A, lanes 9-14), rNF-ATp (Fig. 3A, lanes 17 and 18), or recombinant c-Rel (Fig. 3B, lanes 6-10) to the naked 180-bp fragment of the IL-2 promoter (nt -55 to -235) lead to the formation of specific DNA:protein complexes as would be expected from previous studies (20, 23, 28). Neither AP-1 (Fig.

3A, lanes 3-8), NFATp (Fig. 3A, lanes 15 and 16), nor c-Rel (Fig. 3B, lanes 1-5) was capable of binding to the nucleosome-assembled DNA, even with the addition of up to 10 times the amount of protein required to form specific complexes on naked DNA. The complexes detected in these binding reactions are due to the presence of some free DNA in the nucleosome preparations (Fig. 3, A and B). The reduction in intensity of the nucleosome complex at the highest concentration of AP-1 is most likely due to nonspecific interactions as is also evident in the free DNA lanes (Fig. 3A, lanes 3 and 9). Combinations of these transcription factors were tested for their ability to bind to nucleosome-assembled DNA but no combinations were found that could successfully bind (data not shown). DNase I footprinting experiments confirmed the inability of the transcription factors either alone or in combination to bind to nucleosome-assembled DNA (data not shown).

We have previously demonstrated that the architectural nuclear protein, HMGA1 is important in the assembly of multiprotein complexes on the CD28RR of the IL-2 promoter (20, 28). Because it is known that HMGA1 proteins are able to interact with nucleosome core particles and, consequently, alter the rotational setting of DNA on the nucleosome surface (45, 46, 48), we analyzed HMGA1 interactions with the 180-bp IL-2 promoter fragment assembled into mononucleosomes. When recombinant HMGA1a and HMGA1b proteins were titrated onto the 180-bp IL-2 DNA fragment assembled into nucleosomes, the intensity of the nucleosome complex band decreased and a slower migrating complex (HMG/nuc) appeared (Fig. 4A, lanes 1-6). The specificity of HMGA1 binding was tested by using the non-DNA binding HMGA1a mutant, HMGI-mII,III, which has mutations in the BD II and III domains that are critical for specific DNA interactions (26). As expected, HMGI-mII,III did not bind to the IL-2 nucleosome when used at the same concentrations as HMGA1a and HMGA1b (Fig. 4A, lanes 7-9).

To determine the location of HMGA1 binding to the IL-2 nucleosome complex and to ascertain whether HMGA1 binding can alter the rotational setting of the nucleosome, *in vitro* DNase I footprinting was used. The addition of increasing concentrations of HMGA1a to naked DNA generated specific footprints within the

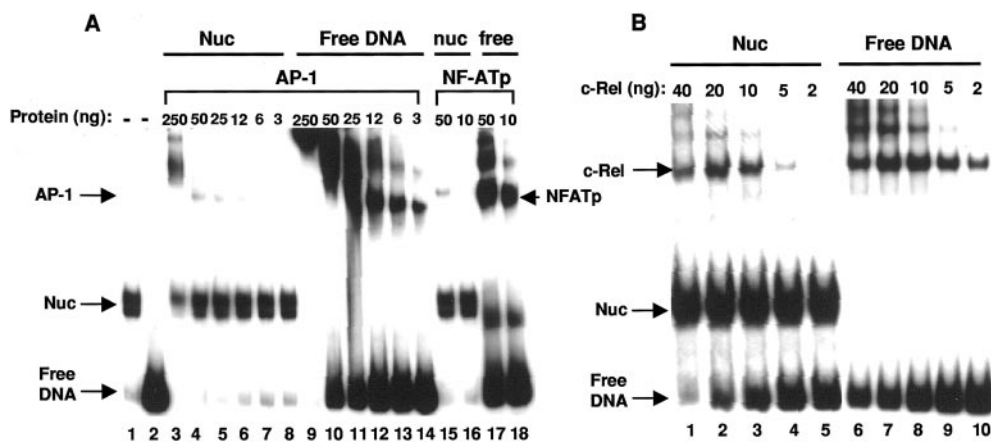
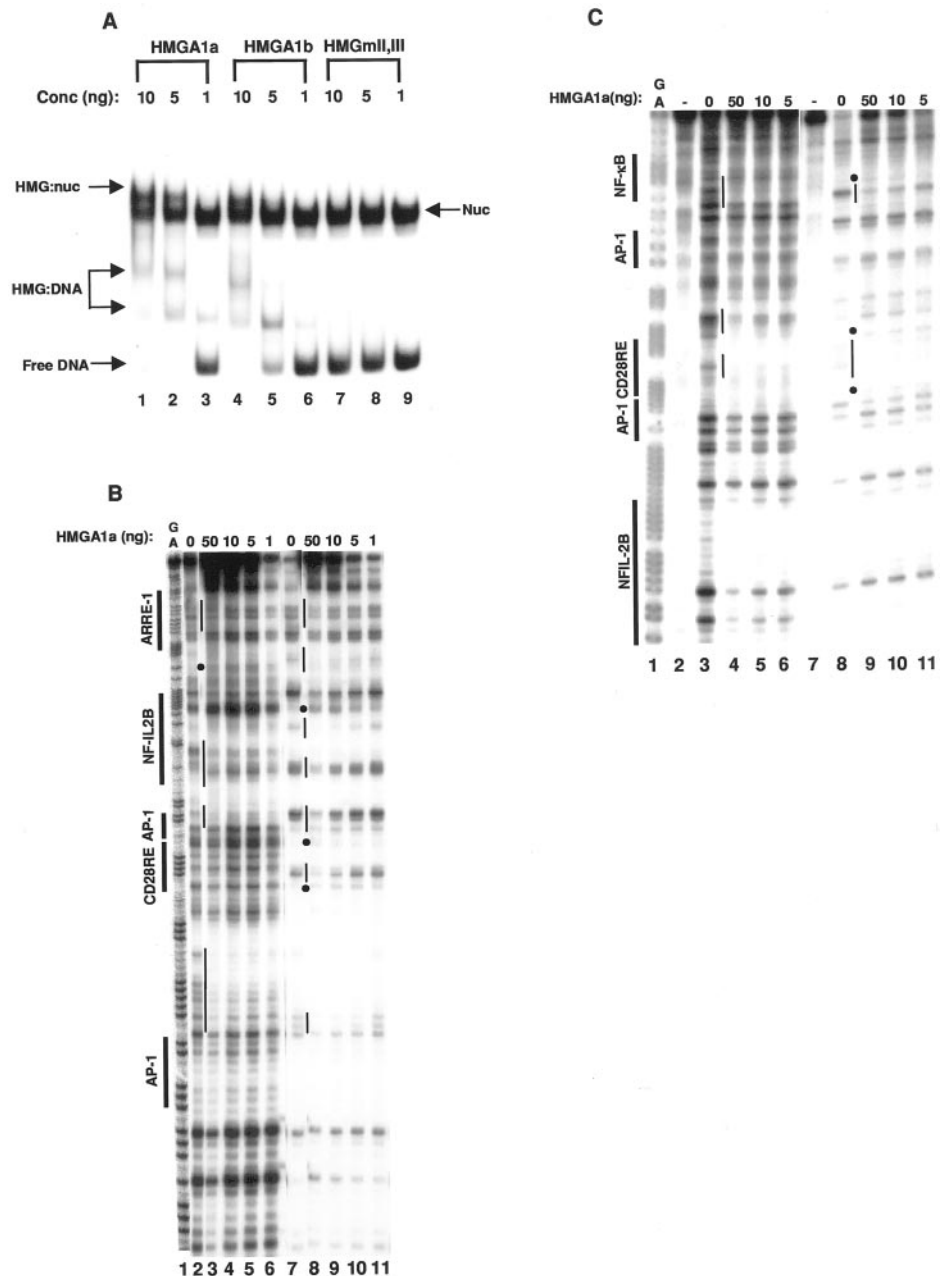


**FIGURE 3.** Transcription factors fail to bind to the IL-2 nucleosome complex. A, AP-1 and NF-ATp fail to bind to the *in vitro*-assembled IL-2 nucleosome complex. Recombinant full-length (*c-fos/c-jun*) AP-1 or NF-ATp protein was incubated with either free DNA or IL-2 nucleosomes in EMSA reactions. Decreasing concentrations (250, 50, 25, 12, 6, and 3 ng) of AP-1 were combined with nucleosomal DNA (lanes 3-8) and free DNA (lanes 9-14). Similarly, 50 and 10 ng of NF-ATp were combined with IL-2 nucleosomes (lanes 15 and 16) and free DNA (lanes 17 and 18). IL-2 nucleosomes alone (lane 1) and free DNA alone (lane 2) were also analyzed. The AP-1 and NF-ATp protein amounts used in the individual lanes are indicated above the lanes. The nucleosome complex, protein/free DNA complexes, and free DNA are indicated. B, c-Rel does not bind to the *in vitro* IL-2 nucleosome. Lanes 1-5 contain decreasing concentrations of recombinant full-length c-Rel (40, 20, 10, 5, and 2 ng) added to IL-2 nucleosomes while lanes 6-10 represent the same amount of c-Rel added to naked DNA. EMSAs and fragment separation were conducted as described above. The nucleosome, free DNA, and protein-free DNA complexes are labeled as above.

**FIGURE 4.** HMGA1 specifically binds to the IL-2 nucleosome. *A*, HMGA1a and HMGA1b bind specifically to the in vitro IL-2 nucleosome. Decreasing concentrations (10, 5, and 1 ng) of recombinant HMGA1a (lanes 1–3), HMGA1b (lanes 4–6), and HMGI-mIL,III (lanes 7–9) were added to the IL-2 nucleosome and complexes separated by nondenaturing gel electrophoresis. The HMG-I protein amounts used in the individual lanes are indicated above the lanes. The nucleosome (Nuc), HMG/nucleosome (HMG:nuc), HMG/free DNA (HMG:DNA), and Free DNA complexes are indicated in the appropriate lanes. *B*, DNase I footprinting analysis of HMGA1a binding to the in vitro IL-2 nucleosome. Free DNA (lanes 3–6) and reconstituted IL-2 nucleosomes (lanes 8–11) were incubated with decreasing amounts (50, 10, 5, and 1 ng) of HMGA1a as indicated. Free DNA (lane 2) and nucleosomal DNA (lane 7) digested with DNase I, but without HMGA1a, are also shown. The G + A sequencing marker is shown in lane 1. Vertical lines indicate the transcription factor binding sites relative to the sequence. Solid lines beside the lanes show the regions of DNA footprinted by HMGA1a whereas dots indicate HMGA1a-induced hypersensitive bands. *C*, Binding of HMG-I to the noncoding strand of nucleosomal DNA. Free DNA (lanes 4–6) and reconstituted IL-2 nucleosomes (lanes 9–11) were incubated with decreasing amounts (50, 10, and 5 ng) of HMGA1a as indicated. Free DNA (lane 3) and nucleosomal DNA (lane 8) was analyzed with DNase I alone. No DNase I was added to lanes 2 and 7. The gel was analyzed and labeled as above.



ARRE-1 region, the NF-IL2B region and the CD28RR (Fig. 4*B*, lanes 3–6) as previously described (28). HMGA1a footprints are also detected at the NF- $\kappa$ B site and CD28RE when the opposite strand is analyzed (Fig. 4*C*, lanes 2–5). When HMGA1a was titrated onto IL-2 nucleosomal DNA, footprints were observed specifically at the ARRE-1, NF-IL2B regions, CD28RR and the NF- $\kappa$ B site (Fig. 4, *B*, lanes 8–11, and *C*, lanes 9–11, refer to lines). At these regions, the presence of HMGA1a also resulted in the reappearance of specific DNase I hypersensitive bands (Fig. 4, *B*, lane 8, and *C*, lane 9, refer to dots) seen in naked DNA and may represent local disruption of the nucleosome:DNA contacts at the specific regions where HMGA1a binds. However, HMGA1 proteins did not appear to alter the rotational setting of the nucleosome nor did they promote the binding of transcription factors such as c-Rel or AP-1 to the nucleosome-assembled IL-2 promoter (data not shown). In summary, all of the transcription factors tested, with the exception of HMGA1, were occluded from binding to the nucleosome-assembled IL-2 promoter. HMGA1 bound to the nucleo-

some-assembled DNA and lead to local but not complete disruption of nucleosome:DNA contacts.

#### *Evidence for a positioned nucleosome at the IL-2 proximal promoter in vivo*

To address whether the IL-2 gene promoter in its native environment in T cell nuclei assembles a positioned nucleosome similar to the in vitro-assembled IL-2 nucleosome, we examined nucleosome organization in vivo using two independent, but complementary, methods: LM-PCR (41) and CHART-PCR (51). The analysis of nucleosome positioning was first performed using LM-PCR and the chemical nuclease, BLM (49). BLM preferentially cleaves linker DNA between nucleosome core particles (49, 50) and has sequence specificity in order of decreasing preference for GC, GT, GA, and AT base pairs (53). Human Jurkat T cells were treated with increasing concentrations of BLM, genomic DNA was isolated, and was then analyzed by LM-PCR using IL-2

promoter-specific primer sets (Fig. 1, set A: 11, 12, 13 and set B: 56, 57, 58).

Densitometric comparisons of cellular (Fig. 5A, lanes 4–7) and naked DNA (Fig. 5A, lanes 2 and 3) damage with bleomycin using a coding strand-specific primer “set A” extending from nt –330 downstream (Fig. 1) indicated that the region of DNA between –190 and +10 was less digested in the cellular DNA than in the naked DNA (Fig. 5A, lanes 2 and 6). Bleomycin-specific bands from cellular DNA occurring at –260 and –270 bp were also significantly reduced in intensity relative to naked DNA (Fig. 5A), indicating that there may be a nucleosome downstream of –190 bp and also at –260 to –270 bp. However, the bleomycin hypersensitive bands at ~–190 and –235 bp were equally represented in both cellular and naked DNA samples indicating an apparent lack of protection in these regions. In addition, clusters of hypersensitive bands of approximately equal intensity occurred from +10 bp toward the coding region of the IL-2 gene in both naked and genomic DNA indicating a possible lack of nucleosomes in this region (Fig. 5A, lanes 2 and 6).

An additional set of coding-strand primers, “set B”, extending from –170 bp downstream toward the start of transcription, was used to further resolve the proximal promoter region closest to the transcriptional start site (Fig. 1). This set of primers shows protected bands from ~–10 extending upstream from the transcription start site (Fig. 5B, compare lanes 3 and 4 with 6–8). Again, the region downstream from the transcription start site was not protected in cellular DNA (Fig. 5B).

The ability of the *HinfI* and *DraI* enzymes as well as MNase to digest the IL-2 proximal promoter in Jurkat T cell nuclei was next examined using the CHART-PCR assay (51). In this assay, the amount of digestion is monitored by real-time PCR using primer sets that amplify ~100 bp and the amount of PCR product is inversely proportional to the amount of digestion. Real-time PCR-using primers encompassing the distal promoter region (set A, nt –595 to –465), the region of the CD28RR (set B, nt –220 to –120) and downstream of the transcription start site (set C, nt +16 to +110) (see Fig. 1), were used to perform the CHART-PCR assay across the IL-2 gene. *DraI* digests the IL-2 promoter at nt –167 close to the CD28RR whereas *HinfI* cleaves at nt –151 between the CD28RE and AP-1 sites within the fragment amplified by primer set B (Fig. 1). Purified genomic DNA used as a control is almost completely digested (95%) within 60 min of exposure to either *HinfI* or *DraI* (Fig. 6A). The IL-2 promoter in nuclear DNA was highly protected from digestion with only ~15% digestion observed in nuclei from unstimulated Jurkat T cells compared with undigested DNA (Fig. 6A). This is not simply an artifact of digestion within the nucleus as the amount of digestion increases with stimulation (see next section and Fig. 7). In addition, the in vitro assembled nucleosome also protects the promoter from restriction enzyme digestion (data not shown). Primer set A was used to monitor nonspecific accessibility because the region amplified by this primer set did not contain a *DraI* or *HinfI* site. Only 3–6% of the DNA was measured as accessible using this primer set (Fig. 6A) implying that only a small amount of nonspecific endonuclease digestion of the DNA is occurring in the experiments.

MNase was also used to assess the chromatin structure of the regions of the IL-2 gene encompassed by primer sets A, B, and C. When nuclei from unstimulated Jurkat T cells were subjected to MNase digestion, the proximal promoter region of the gene, as assessed by primer set B, was the least accessible to digestion (Fig. 6B).

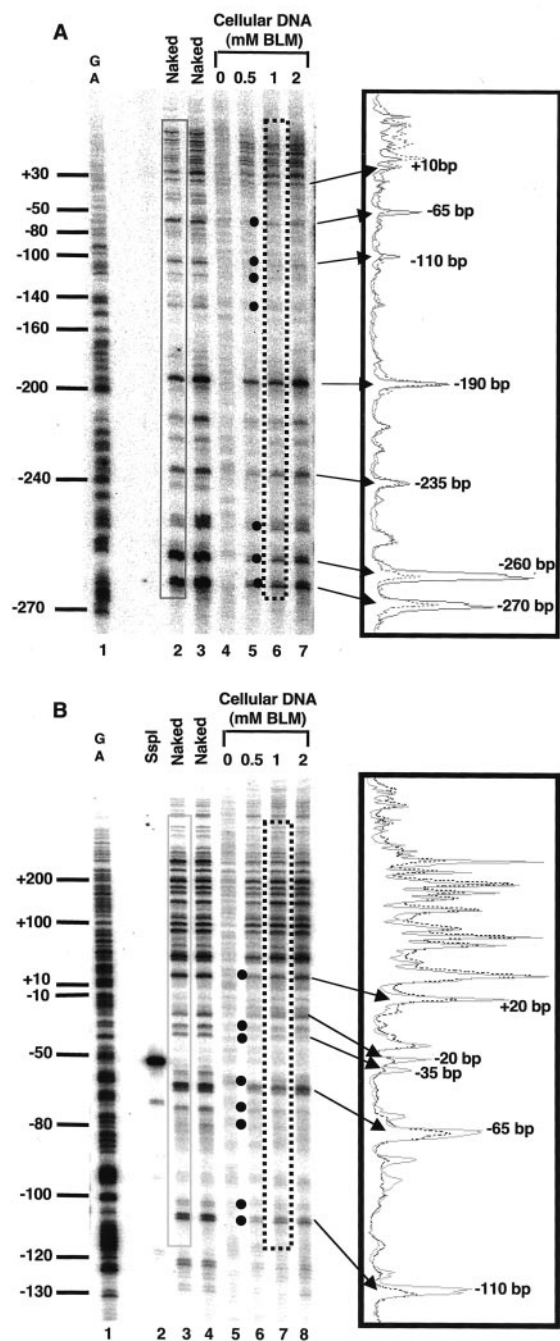


**FIGURE 5.** Identification of a potential nucleosome footprint at the proximal IL-2 promoter in vivo. Unstimulated Jurkat T cells were treated with increasing concentrations (0.5, 1, and 2 mM) of BLM and isolated genomic DNA was analyzed for footprints with coding primer set A (A) or primer set B (B) using LM-PCR. Lanes 5–7 (A) or lanes 6–8 (B) contained purified genomic DNA from BLM-treated Jurkat T cells and DNA without BLM added was analyzed in lane 4 (A) or lane 5 (B). Lanes 2 and 3 (A) or 3 and 4 (B) contained genomic DNA treated with BLM (4  $\mu$ M) in vitro and a G + A sequencing reaction is shown in lane 1. Black dots highlight the location of bands with decreased intensity in the cellular DNA lanes. Lanes 2 and 6 (A) and lanes 3 and 7 (B) were scanned using ImageGauge software resulting in the densitometry graphs shown inside the boxes. Sequence positions of major BLM-sensitive bands on the IL-2 promoter are indicated on the scans.

Taken together, these bleomycin, restriction enzyme, and MNase protection data provide evidence for the presence of a nucleosome(s) across the proximal promoter of the IL-2 gene in unstimulated Jurkat

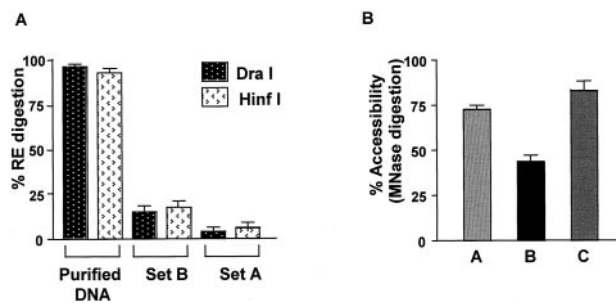


**FIGURE 6.** Accessibility of the IL-2 promoter region to nucleases. *A*, Comparison of restriction enzyme-digested DNA in vitro and in vivo using CHART-PCR. Purified genomic DNA was incubated with either *DraI* or *HinfI* for 60 min at 37°C. Unstimulated (NS) Jurkat T cell nuclei were incubated with either 200 U of *DraI* or *HinfI* for 60 min at 37°C. Genomic DNA (50 ng) was subjected to SYBR Green real-time PCR analysis using primer set B. Primer set A was used to measure background accessibility in *DraI* or *HinfI*-treated nuclei. The Ct values generated were converted to DNA concentration using the standard curve generated from a titration of genomic DNA. The *DraI* or *HinfI* accessibility was expressed as a percentage of uncut DNA and is plotted for purified DNA and cellular DNA. *B*, The IL-2 promoter shows the lowest accessibility to MNase in vivo. Intact nuclei, isolated from unstimulated Jurkat T cells were incubated with or without 50 U MNase for 5 min at RT. Genomic DNA (50 ng) was subjected to SYBR Green real-time PCR analysis using primer sets A, B, and C. The Ct values generated were converted to DNA concentration using a standard curve. The MNase accessibility was expressed as a percentage of the nonstimulated undigested genomic DNA samples. Data shown are means and SE of three separate experiments.

T cells. However, regions outside the proximal promoter may not be as strongly protected by nucleosomes.

#### *Chromatin across the IL-2 proximal promoter is remodeled upon T cell activation*

Because the IL-2 gene is a highly inducible gene, becoming rapidly expressed upon T cell activation, we next asked whether alterations occur in chromatin structure across the proximal promoter upon activation of the cell. Chromatin remodeling of the IL-2 proximal promoter was examined in vivo using restriction enzyme and MNase digestion with the CHART-PCR assay (51). In unstimulated Jurkat T cells, we observed a low level of accessibility to *DraI* and *HinfI* (~15%) when compared with undigested DNA from unstimulated cells as described above (Fig. 6A). Increases in *DraI* accessibility were first observed in cells stimulated for 1 h and continued to increase with a maximum reached at 3 h of stimulation (Fig. 7, *A* and *B*, ~50% in PMA/I-treated cells and 70% in cells treated with PMA/I +  $\alpha$ -CD28). By 4 and 8 h post-stimulation, the amount of *DraI* accessibility decreased to ~25% relative to unstimulated cells. As a control, a region of the promoter lacking a *DraI* site (set A) was analyzed in unstimulated and stimulated cells over the time period and as anticipated, there was no change in accessibility in all samples (Fig. 6A; data not shown). The time course of *HinfI* accessibility followed that of *DraI* with the exception that accessibility was observed as early as 30 min following activation (Fig. 7, *A* and *B*). When the time course of chromatin accessibility with *DraI* or *HinfI* was plotted with the time course of IL-2 mRNA production measured by real-time PCR, it is clear that chromatin accessibility reaches a maximum ~1 h before the maximum accumulation of IL-2 mRNA (Fig. 7, *C* and *D*). These data suggest that chromatin remodeling is a prerequisite for maximal expression of the IL-2 gene.

Changes in MNase accessibility were also measured across the IL-2 gene with the CHART-PCR assay and the three sets of prim-

ers shown in Fig. 1. PMA/I activation resulted in only a small change in MNase accessibility across the primer set B region (Fig. 7E) but PMA/I + CD28 activation led to almost a 2-fold increase in accessibility across this region (Fig. 7E). The regions of the gene assayed by primer sets A (-595 to -465) and C (+15 to +110) showed little change in MNase accessibility following activation (Fig. 7E).

These results suggest that chromatin remodeling is occurring across the proximal promoter region of the human IL-2 gene following activation. The region of remodeling corresponds to the region that can assemble a positioned nucleosome in vitro and where a nucleosome is also likely to exist in vivo.

## Discussion

In this study, we report that the proximal promoter region of the IL-2 gene is able to assemble into a rotationally and translationally positioned mononucleosome under chromatin reconstitution conditions in vitro and critical regulatory elements including the ARRE-1, NF-IL2B, and CD28RR sites are contained within its translational boundaries. This is in contrast to the GM-CSF promoter which does not appear to assemble a highly positioned nucleosome. In fact only a few DNA fragments have been shown to assemble such a highly positioned nucleosome with the most widely used example being the 5S RNA positioning sequences (54, 55). Numerous studies on DNA sequences required for nucleosome positioning have revealed that highly flexible poly(A-T) DNA assembles nucleosomes more readily than bulk DNA (54, 56–60). Subsequently, these studies have determined that the artificial repeat sequence TATAACGCC has the highest affinity for binding nucleosomes and assembles highly positioned nucleosomes (61). This is probably due to the alternating A/T and G/C rich elements in phase with the helical repeat, which provides a flexible sequence that can cope with the torsional stress when associated with nucleosomes. The proximal promoter sequence of IL-2 has a high A/T content (~65%) compared with other inducible cytokine genes (for example, the GM-CSF promoter has 48% A/T content). Interestingly, there is a notable 10–20 bp periodicity of A/T stretches throughout much of the IL-2 minimal promoter region, which could potentially place this sequence in the nucleosome positioning class of DNA fragments containing “TATA-tetrads” (57).

The fact that the in vitro-assembled nucleosome inhibited the binding of CD28RR-specific transcription factors to their DNA binding sites supports a role for this nucleosome in transcriptional repression of the IL-2 gene in resting Jurkat T cells. Interestingly, HMGA1 proteins were found to specifically bind to the ARRE-1, NF-IL2B, CD28RR, and NF- $\kappa$ B sites in the presence of the nucleosome causing local disruption of core particle DNA interactions but not complete nucleosome disruption. However, the binding of HMGA1 did not alter accessibility of restriction enzyme recognition sequences occluded by the positioned nucleosome nor did it promote transcription factor binding to these core particles in vitro (data not shown). Therefore, these data suggest that additional processes, besides HMGA1 binding to the IL-2 nucleosome, are needed for the subsequent chromatin remodeling which takes place when cells are activated.

Interestingly, the chromatin structure of the promoter of the human IL-2R $\alpha$  gene shares many similarities to that of the IL-2 promoter reported in this study. In vitro IL-2R $\alpha$  promoter DNA assembles a stably positioned nucleosome and there is evidence for nucleosome remodeling of this region of the promoter during transcriptional activation of the gene (62). In addition, HMGA1 has recently been shown to bind directionally to the IL-2R $\alpha$  promoter when it is assembled into nucleosomes (62). Reeves et al. (62)

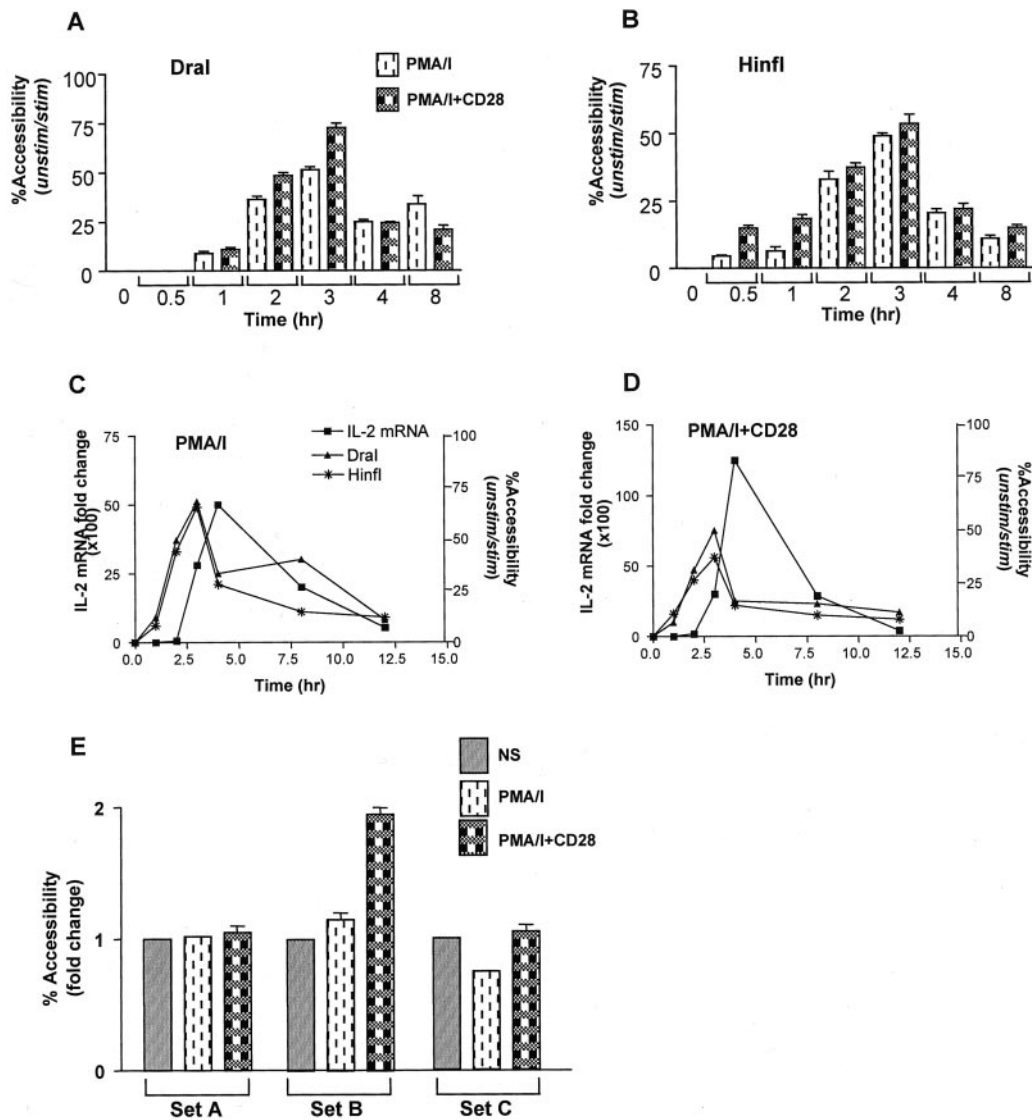


**FIGURE 7.** CHART-PCR analysis of chromatin remodeling at the IL-2 proximal promoter region in vivo. *A* and *B*, *DraI* and *HinfI* restriction enzyme accessibility kinetics in activated Jurkat T cells. Nuclei prepared from Jurkat T cells unstimulated or stimulated with P/I and P/I/CD28 for the time points indicated were incubated with either 200 U *DraI* (*A*) or *HinfI* (*B*) for 60 min at 37°C. Genomic DNA (50 ng) from each sample was subjected to SYBR Green real-time PCR analysis using primer set B. The Ct values generated were converted to DNA concentration using a standard curve. The *DraI* and *HinfI* accessibility in the stimulated cells was expressed as a percentage of digested DNA from unstimulated cells. *C* and *D*, Comparison of IL-2 remodeling kinetics and IL-2 mRNA expression. Accessibility data from both P/I (*C*) and P/I/CD28 (*D*) stimulated cells using primer set B and IL-2 mRNA kinetics measured by SYBR Green real-time PCR with primer set C are plotted together. IL-2 mRNA levels are plotted as fold change relative to the unstimulated sample. Data shown are means for three separate experiments. *E*, Changes in MNase accessibility across the IL-2 gene. Nuclei from unstimulated or P/I or P/I + CD28-stimulated cells were subjected to limited MNase digestion and the isolated genomic DNA was analyzed by real-time PCR using primer sets A, B, and C. The percentage of MNase digestion is presented relative to that observed in unstimulated MNase-digested cells which is given a value of 1 for each primer set.

proposed that HMGA1 may form part of a targeting signal to recruit chromatin remodeling complexes to the IL-2R $\alpha$  promoter. It is intriguing that two genes whose products are critical for the correct activation of T cells can assemble highly positioned nucleosomes across their promoter regions which bind HMGA1, and presumably function to prevent inadvertent transcription from these genes unless the correct activation signals are present.

Chromatin accessibility data derived from in vivo genomic footprinting by LM-PCR as well as restriction enzyme and MNase accessibility by CHART-PCR provides evidence for the presence of a nucleosome on the IL-2 promoter in resting Jurkat T cells. We have recently examined the chromatin structure of the mouse IL-2 promoter in EL-4 T cells and CD4<sup>+</sup> primary T cells and find a

complete lack of MNase or RE accessibility across the proximal promoter in these cells before stimulation (51), again supporting the idea that the IL-2 promoter is assembled into nucleosomes. Bleomycin-LM-PCR footprinting data suggested that a nucleosome plus perhaps additional promoter binding factors may be located in the region from  $\sim -15$  to  $-190$  bp. The location of the in vitro-positioned nucleosome ( $-60$  to  $-210$ ) lies approximately within the bleomycin-footprinted region suggesting that the bleomycin footprint may in part represent a positioned nucleosome. It has previously been shown that a constitutive DNase I footprint occurs across the TATA box region of the IL-2 promoter in Jurkat T cells and this has been interpreted as representing a paused polymerase complex (40, 41). Such a complex together with a

nucleosome could explain the size of the observed bleomycin footprint.

In this study, we show, using the CHART-PCR assay with restriction enzyme or MNase accessibility, that the chromatin structure of the proximal promoter region, but not other regions of the IL-2 gene, is remodeled following T cell activation. Time course experiments of the accessibility changes within the IL-2 proximal promoter showed a gradual rise in RE accessibility from 30 min to 3 h following activation. This gradual change in accessibility is in contrast to our experiments with the mouse IL-2 gene where accessibility is not observed until 1.5 h following activation in either EL-4 or primary CD4<sup>+</sup> T cells from mouse spleen and at this time point almost complete accessibility is observed (51). It is possible that the nucleosomes across the proximal promoter region in Jurkat T cells are already modified in some manner. This possibility is consistent with the observation that the mouse gene appears to be completely inaccessible to MNase or RE digestion in resting cells (51), while the human gene, at least in Jurkat T cells, has a higher level of intrinsic accessibility especially to MNase digestion. The distinct time course of chromatin accessibility change is reflected in distinct time courses of IL-2 mRNA synthesis for Jurkat and EL-4 cells. However, in both cases, the time of chromatin remodeling precedes the time of mRNA accumulation implying that chromatin remodeling may be a prerequisite for high levels of gene transcription.

There also appears to be some differences in the signals required for chromatin remodeling across the IL-2 promoter in Jurkat T cells and EL-4 cells. In EL-4 cells, P/I leads to almost complete accessibility with a small contribution from CD28 for either restriction enzyme accessibility or MNase accessibility (51). In addition, PMA alone is almost as effective as P/I (51). However, in Jurkat cells while P/I increases restriction enzyme accessibility, it has little effect on MNase accessibility and CD28 signaling is required to generate MNase accessibility. It is unclear why these differences exist but may relate to the higher level of MNase accessibility seen in unstimulated Jurkat T cells compared with EL-4s as discussed below.

The higher constitutive accessibility of the human gene in Jurkat T cells compared with the mouse gene in EL-4 and primary T cells and the faster kinetics of chromatin remodeling and mRNA accumulation may relate to the recent finding that the D3 phosphoinositide phosphatase and tensin homolog is deficient in Jurkat T cells (63). As a consequence, there are elevated levels of the phosphoinositol 3-kinase products, PI-3,4-P<sub>2</sub> and PI-3,4,5-P<sub>3</sub>, in the plasma membrane leading to constitutive recruitment of pleckstrin homology domain proteins such as Itk (63). Thus, constitutive signaling through this pathway could contribute to the more accessible chromatin structure on the IL-2 gene and the faster response to activation. Indeed, it has been shown that phospholipids are involved in the targeting of the BAF chromatin remodeling complex to chromatin following T cell activation (64).

In summary, we suggest that chromatin is a necessary component of IL-2 gene regulation. A highly positioned nucleosome most likely exists across the proximal promoter region of the IL-2 gene in vivo preventing transcription factor binding in the absence of a stimulus that triggers chromatin remodeling. Although HMGA1 can bind to its recognition sites in the presence of a nucleosome it is not sufficient to promote transcription factor binding or to lead to complete disruption of the nucleosome. An understanding of the signals and molecules required for disruption of this nucleosome in vivo will help to further elucidate the role of chromatin in IL-2 gene transcription.

## Acknowledgments

We thank M. Nissen for excellent technical assistance, S. Rao for assistance with CHART-PCR assays, and L. Beckerbauer, N. Treff, G. Dement, and D. Edberg for helpful comments on the work and manuscript.

## References

- Gaffen, S. L. 2001. Signaling domains of the interleukin 2 receptor. *Cytokine* 14:63.
- Smith, K. A. 1992. Interleukin-2. *Curr. Opin. Immunol.* 4:271.
- Rudd, C. E. 1996. Upstream-downstream: CD28 cosignaling pathways and T cell function. *Immunity* 4:527.
- Reya, T., H. Bassiri, R. Biancaniello, and S. R. Carding. 1998. Thymic stromal-cell abnormalities and dysregulated T-cell development in IL-2-deficient mice. *Dev. Immunol.* 5:287.
- Razi-Wolf, Z., G. A. Hollander, and H. Reiser. 1996. Activation of CD4<sup>+</sup> T lymphocytes form interleukin 2-deficient mice by costimulatory B7 molecules. *Proc. Natl. Acad. Sci. USA* 93:2903.
- Hollander, G. A. 1999. On the stochastic regulation of interleukin-2 transcription. *Semin. Immunol.* 11:357.
- Shaw, J., K. Meerovitch, R. C. Bleackley, and V. Paetkau. 1988. Mechanisms regulating the level of IL-2 mRNA in T lymphocytes. *J. Immunol.* 140:2243.
- Fraser, J. D., M. E. Newton, and A. Weiss. 1992. CD28 and T cell antigen receptor signal transduction coordinately regulate interleukin 2 gene expression in response to superantigen stimulation. *J. Exp. Med.* 175:1131.
- Durand, D. B., M. R. Bush, J. G. Morgan, A. Weiss, and G. R. Crabtree. 1987. A 275 basepair fragment at the 5' end of the interleukin 2 gene enhances expression from a heterologous promoter in response to signals from the T cell antigen receptor. *J. Exp. Med.* 165:395.
- Fujita, T., H. Shibuya, T. Ohashi, K. Yamanishi, and T. Taniguchi. 1986. Regulation of human interleukin-2 gene: functional DNA sequences in the 5' flanking region for the gene expression in activated T lymphocytes. *Cell* 46:401.
- Durand, D. B., J. P. Shaw, M. R. Bush, R. E. Replogle, R. Belagaje, and G. R. Crabtree. 1988. Characterization of antigen receptor response elements within the interleukin-2 enhancer. *Mol. Cell. Biol.* 8:1715.
- Ullman, K. S., W. M. Flanagan, C. A. Edwards, and G. R. Crabtree. 1991. Activation of early gene expression in T lymphocytes by Oct-1 and an inducible protein, OAP40. *Science* 254:558.
- Ullman, K. S., J. P. Northrop, A. Admon, and G. R. Crabtree. 1993. Jun family members are controlled by a calcium-regulated, cyclosporin A-sensitive signaling pathway in activated T lymphocytes. *Genes Dev.* 7:188.
- Jain, J., P. G. McCaffrey, V. E. Valge-Archer, and A. Rao. 1992. Nuclear factor of activated T cells contains Fos and Jun. *Nature* 356:801.
- Boise, L. H., B. Petryniak, X. Mao, C. H. June, C. Y. Wang, T. Lindsten, R. Bravo, K. Kovary, J. M. Leiden, and C. B. Thompson. 1993. The NFAT-1 DNA binding complex in activated T cells contains Fra-1 and JunB. *Mol. Cell. Biol.* 13:1911.
- Brabletz, T., I. Pietrowski, and E. Serfling. 1991. The immunosuppressives FK 506 and cyclosporin A inhibit the generation of protein factors binding to the two purine boxes of the interleukin 2 enhancer. *Nucleic Acids Res.* 19:61.
- Rooney, J. W., Y. L. Sun, L. H. Glimcher, and T. Hoey. 1995. Novel NFAT sites that mediate activation of the interleukin-2 promoter in response to T-cell receptor stimulation. *Mol. Cell. Biol.* 15:6299.
- Verweij, C. L., M. Geerts, and L. A. Aarden. 1991. Activation of interleukin-2 gene transcription via the T-cell surface molecule CD28 is mediated through an NF- $\kappa$ B-like response element. *J. Biol. Chem.* 266:14179.
- Serfling, E., A. Avots, and M. Neumann. 1995. The architecture of the interleukin-2 promoter: a reflection of T lymphocyte activation. *Biochim. Biophys. Acta* 1263:181.
- Himes, S. R., L. S. Coles, R. Reeves, and M. F. Shannon. 1996. High mobility group protein I(Y) is required for function and for c-Rel binding to CD28 response elements within the GM-CSF and IL-2 promoters. *Immunity* 5:479.
- Bryan, R. G., Y. Li, J. H. Lai, M. Van, N. R. Rice, R. R. Rich, and T. H. Tan. 1994. Effect of CD28 signal transduction on c-Rel in human peripheral blood T cells. *Mol. Cell. Biol.* 14:7933.
- McGuire, K. L., and M. Iacobelli. 1997. Involvement of Rel, Fos, and Jun proteins in binding activity to the IL-2 promoter CD28 response element/AP-1 sequence in human T cells. *J. Immunol.* 159:1319.
- Shang, C., J. Attema, D. Cakouros, P. N. Cockerill, and M. F. Shannon. 1999. Nuclear factor of activated T cells contributes to the function of the CD28 response region of the granulocyte macrophage-colony stimulating factor promoter. *Int. Immunol.* 11:1945.
- Shapiro, V. S., K. E. Truitt, J. B. Imboden, and A. Weiss. 1997. CD28 mediates transcriptional upregulation of the interleukin-2 (IL-2) promoter through a composite element containing the CD28RE and NF-IL-2B AP-1 sites. *Mol. Cell. Biol.* 17:4051.
- Butscher, W. G., C. Powers, M. Olive, C. Vinson, and K. Gardner. 1998. Coordinate transactivation of the interleukin-2 CD28 response element by c-Rel and ATF-1/CREB2. *J. Biol. Chem.* 273:552.
- Parra, E., K. McGuire, G. Hedlund, and M. Dohlsten. 1998. Overexpression of p65 and c-Jun substitutes for B7-1 costimulation by targeting the CD28RE within the IL-2 promoter. *J. Immunol.* 160:5374.
- Reeves, R., and L. Beckerbauer. 2001. HMGI/Y proteins: flexible regulators of transcription and chromatin structure. *Biochim. Biophys. Acta* 1519:13.

28. Himes, S. R., R. Reeves, J. Attema, M. Nissen, Y. Li, and M. F. Shannon. 2000. The role of high-mobility group I(Y) proteins in expression of IL-2 and T cell proliferation. *J. Immunol.* 164:3157.
29. Paranjape, S. M., R. T. Kamakaka, and J. T. Kadonaga. 1994. Role of chromatin structure in the regulation of transcription by RNA polymerase II. *Annu. Rev. Biochem.* 63:265.
30. Wolffe, A. P. 1995. Centromeric chromatin: histone deviants. *Curr. Biol.* 5:452.
31. Workman, J. L., and R. E. Kingston. 1998. Alteration of nucleosome structure as a mechanism of transcriptional regulation. *Annu. Rev. Biochem.* 67:545.
32. Wolffe, A. P. 1994. Nucleosome positioning and modification: chromatin structures that potentiate transcription. *Trends Biochem. Sci.* 19:240.
33. Weinmann, A. S., S. E. Plevy, and S. T. Smale. 1999. Rapid and selective remodeling of a positioned nucleosome during the induction of IL-12 p40 transcription. *Immunity* 11:665.
34. Ng, K. W., P. Ridgway, D. R. Cohen, and D. J. Tremethick. 1997. The binding of a Fos/Jun heterodimer can completely disrupt the structure of a nucleosome. *EMBO J.* 16:2072.
35. Korner, K., and R. Muller. 2000. In vivo structure of the cell cycle-regulated human cdc25C promoter. *J. Biol. Chem.* 275:18676.
36. Belikov, S., B. Gelius, and O. Wrangé. 2001. Hormone-induced nucleosome positioning in the MMTV promoter is reversible. *EMBO J.* 20:2802.
37. Garrity, P. A., D. Chen, E. V. Rothenberg, and B. J. Wold. 1994. Interleukin-2 transcription is regulated in vivo at the level of coordinated binding of both constitutive and regulated factors. *Mol. Cell. Biol.* 14:2159.
38. Rothenberg, E. V., and S. B. Ward. 1996. A dynamic assembly of diverse transcription factors integrates activation and cell-type information for interleukin 2 gene regulation. *Proc. Natl. Acad. Sci. USA* 93:9358.
39. Ward, S. B., G. Hernandez-Hoyos, F. Chen, M. Waterman, R. Reeves, and E. V. Rothenberg. 1998. Chromatin remodeling of the interleukin-2 gene: distinct alterations in the proximal versus distal enhancer regions. *Nucleic Acids Res.* 26:2923.
40. Siebenlist, U., D. B. Durand, P. Bressler, N. J. Holbrook, C. A. Norris, M. Kamoun, J. A. Kant, and G. R. Crabtree. 1986. Promoter region of interleukin-2 gene undergoes chromatin structure changes and confers inducibility on chloramphenicol acetyltransferase gene during activation of T cells. *Mol. Cell. Biol.* 6:3042.
41. Brunvand, M. W., A. Krumm, and M. Groudine. 1993. In vivo footprinting of the human IL-2 gene reveals a nuclear factor bound to the transcription start site in T cells. *Nucleic Acids Res.* 21:4824.
42. Abate, C., D. Luk, R. Gentz, F. J. Rauscher III, and T. Curran. 1990. Expression and purification of the leucine zipper and DNA-binding domains of Fos and Jun: both Fos and Jun contact DNA directly. *Proc. Natl. Acad. Sci. USA* 87:1032.
43. Reeves, R., and M. S. Nissen. 1999. Purification and assays for high mobility group HMG-I(Y) protein function. *Methods Enzymol.* 304:155.
44. Ausubel, F. R., R. Kingston, D. Moore, J. Seidman, J. Smith, and J. Struhl. 1988. *Current Protocols in Molecular Biology*. Wiley, New York.
45. Tatchell, K., and K. E. Van Holde. 1977. Reconstitution of chromatin core particles. *Biochemistry* 16:5295.
46. Yonezawa, A., and Y. Sugiura. 1994. DNA binding mode of class-IIIS restriction endonuclease FokI revealed by DNA footprinting analysis. *Biochim. Biophys. Acta* 1219:369.
47. Reeves, R., and A. P. Wolffe. 1996. Substrate structure influences binding of the non-histone protein HMG-I(Y) to free nucleosomal DNA. *Biochemistry* 35:5063.
48. Hayes, J. J., T. D. Tullius, and A. P. Wolffe. 1990. The structure of DNA in a nucleosome. *Proc. Natl. Acad. Sci. USA* 87:7405.
49. Cairns, M. J., and V. Murray. 1996. Influence of chromatin structure on bleomycin-DNA interactions at base pair resolution in the human  $\beta$ -globin gene cluster. *Biochemistry* 35:8753.
50. Temple, M. D., M. J. Cairns, A. Kim, and V. Murray. 1999. Protein-DNA footprinting of the human epsilon-globin promoter in human intact cells using nitrogen mustard analogues and other DNA-damaging agents. *Biochim. Biophys. Acta* 1445:245.
51. Rao, A., E. Procko, and M. F. Shannon. 2001. Chromatin remodeling, measured by a real-time polymerase chain reaction assay, across the proximal promoter region of the IL-2 gene. *J. Immunol.* 167:4494.
52. Adams, C. C., and J. L. Workman. 1995. Binding of disparate transcriptional activators to nucleosomal DNA is inherently cooperative. *Mol. Cell. Biol.* 15:1405.
53. Hiraku, Y., S. Oikawa, K. Kuroki, H. Sugiyama, I. Saito, and S. Kawanishi. 2001. Amplification of bleomycin-induced DNA cleavage at cytosine residues 3' to GGG sequences by pyrrole triamide. *Biochem. Pharmacol.* 61:351.
54. Shrader, T. E., and D. M. Crothers. 1989. Artificial nucleosome positioning sequences. *Proc. Natl. Acad. Sci. USA* 86:7418.
55. Dong, F., J. C. Hansen, and K. E. van Holde. 1990. DNA and protein determinants of nucleosome positioning on sea urchin 5S rRNA gene sequences in vitro. *Proc. Natl. Acad. Sci. USA* 87:5724.
56. Drew, H. R., and A. A. Travers. 1985. DNA bending and its relation to nucleosome positioning. *J. Mol. Biol.* 186:773.
57. Widlund, H. R., H. Cao, S. Simonsson, E. Magnusson, T. Simonsson, P. E. Nielsen, J. D. Kahn, D. M. Crothers, and M. Kubista. 1997. Identification and characterization of genomic nucleosome-positioning sequences. *J. Mol. Biol.* 267:807.
58. Widlund, H. R., J. M. Vitolo, C. Thiriet, and J. J. Hayes. 2000. DNA sequence-dependent contributions of core histone tails to nucleosome stability: differential effects of acetylation and proteolytic tail removal. *Biochemistry* 39:3835.
59. Pemberton, I. K., G. Muskhelishvili, A. A. Travers, and M. Buckle. 2000. The G+C-rich discriminator region of the *tyrT* promoter antagonises the formation of stable preinitiation complexes. *J. Mol. Biol.* 299:859.
60. Anselmi, C., G. Bocchinfuso, P. De Santis, M. Savino, and A. Scipioni. 2000. A theoretical model for the prediction of sequence-dependent nucleosome thermodynamic stability. *Biophys. J.* 79:601.
61. Widlund, H. R., P. N. Kuduvali, M. Bengtsson, H. Cao, T. D. Tullius, and M. Kubista. 1999. Nucleosome structural features and intrinsic properties of the TATAAACGCC repeat sequence. *J. Biol. Chem.* 274:31847.
62. Reeves, R., W. J. Leonard, and M. S. Nissen. 2000. Binding of HMG-I(Y) imparts architectural specificity to a positioned nucleosome on the promoter of the human interleukin-2 receptor  $\alpha$  gene. *Mol. Cell. Biol.* 20:4666.
63. Shan, X., M. J. Czar, S. C. Bunnell, P. Liu, Y. Liu, P. L. Schwartzberg, and R. L. Wange. 2000. Deficiency of PTEN in Jurkat T cells causes constitutive localisation of Itk to the plasma membrane and hyperresponsiveness to CD3 stimulation. *Mol. Cell. Biol.* 20:6945.
64. Zhao, K., W. Wang, O. J. Rando, Y. Xue, K. Swiderek, A. Kuo, and G. R. Crabtree. 1998. Rapid and phosphoinositide-dependent binding of the SWI/SNF-like BAF complex to chromatin after T lymphocyte receptor signaling. *Cell* 95:625.